JOURNAL OF OPTOELECTRONICS AND ADVANCED MATERIALS, Vol. 11, No. 8, August 2009, p. 1071 - 1076

Interaction of laser radiation with Au nanoparticles in SiO_2 thin films

M. SENDOVA-VASSILEVA[a*], M. SENDOVA[b], H. HOFMEISTER[c], J. C. PIVIN[d]
[a]*Central Laboratory of Solar Energy and New Energy Sources, Bulgarian Academy of Sciences, 72 Tzarigradsko Chaussee Blvd., 1784 Sofia, Bulgaria*
[b]*New College of Florida, 5800 Bay Shore Road, Sarasota, FL 34243-2109, USA*
[c]*Max Planck Institute for Microstructure Physics, Weinberg 2, D-06120 Halle, Germany*
[d]*CSNSM, CNRS, Bâtiment 108, 91405 Orsay Campus, France*

Thin films of SiO_2 containing gold nanoparticles were prepared by magnetron co-sputtering followed by thermal annealing. The samples were irradiated with a pulsed Nd:YAG laser to study the possibility of modifying the nanoparticle size distribution. A small, but observable increase of the mean size of the particles and of the number of larger particles was observed. The surface roughness of the films increased and ripples on the surface were formed after laser irradiation. The growth of the particles was attributed to photostimulated Ostwald ripening. The effects of the laser irradiation on the film are discussed.

(Received February 9, 2009; accepted July 31, 2009)

Keywords: Surface plasmons, Surface roughness, Ostwald ripening, Metal nanoparticles, Thin films

1. Introduction

The interaction between laser radiation and gold nanoparticles has been the subject of many publications most of which deal with gold nanoparticles dispersed in a liquid solution. For example, in [1] hydrosols containing monodisperse gold nanoparticles with mean sizes between 4 and 106 nm were subjected to irradiation with the second and third harmonic of a Nd:YAG: laser. It was found that this leads to fragmentation of larger particles but for particles with a diameter about and smaller than 5 nm, the mean size after laser treatment did not change or even increased a little. Other authors like Satoh et al. [2] dealt with the coagulation and coalescence of gold nanoparticles dispersed in organic liquids subjected to illumination with visible and UV light. They found that the coalescence, i.e. growth in size of the separate particles proceeded through a process similar to Ostwald ripening stimulated by UV irradiation of the solution. On the other hand, the coagulation of the particles, i.e. their grouping together to form a larger structure, was stimulated by visible light which lead to the deionization of the clusters and the increase of the van der Waals forces between them. However, the experimental studies of laser treatment of gold nanoparticles embedded in a solid matrix are scarce. There are several publications where gold particles were used as defect centres in a dielectric matrix in order to study the role of defects in laser induced damage of optically transparent materials [3,4]. The role of gold nanoparticles as plasmonic nanoheaters was studied in an experiment of ice melting [5].

In this paper we study the response of gold nanoparticles embedded in a thin film silica matrix to laser treatment. We have made similar studies on silver nanoparticles [6,7] in the context of the possible applications of dielectric matrices containing noble metal nanoparticles as materials exhibiting optical non-linearity. Such applications would require the use of lasers and the radiation stability of devices would be of primary importance. On the other hand, we have found in previous studies that laser treatment can alter the size distributions of metal nanoparticles embedded in dielectric matrices and possibly make them narrower.

2. Experimental

Thin films of SiO_2 containing Au were prepared by rf magnetron co-sputtering in Ar atmosphere. Pieces of Au wire were placed on the SiO_2 target. The samples were deposited on silica and silicon substrates. In order to prepare films containing bigger metal particles the samples were annealed in air at 950°C for 1 or 5 hours. The Au content in the films was determined by RBS. The laser treatment was performed using a pulsed Nd: YAG laser's 2nd (532 nm; 2.33 eV) and 4th (266 nm; 4.66 eV) harmonic. The pulse width was 5 ns with a repetition rate of 10 Hz and the applied fluences were 35 to 125 mJ/cm^2 per pulse. The beam diameter was 0.5 cm and the scan velocity - 8 μm/s, so that an area of 0.5 cm^2 was irradiated uniformly. The laser beam was linearly polarized.

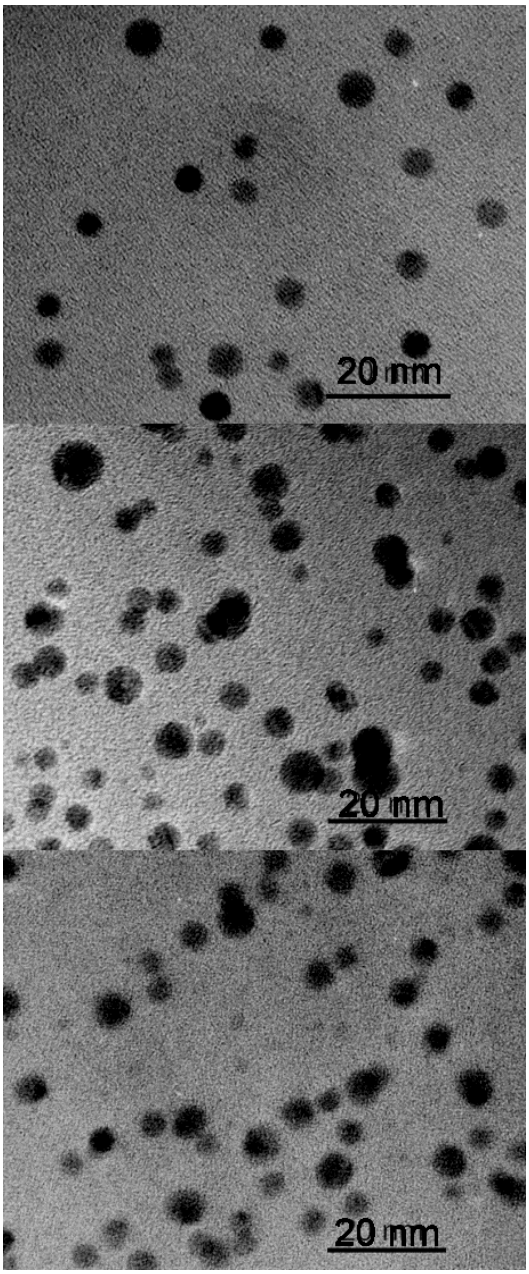

Fig. 1. Example TEM images of Au particles in Sample 1 for (from top to bottom) before laser treatment; after laser treatment with 532 nm at 100 mJ/cm^2; after laser treatment with 266 nm at 50 mJ/cm^2

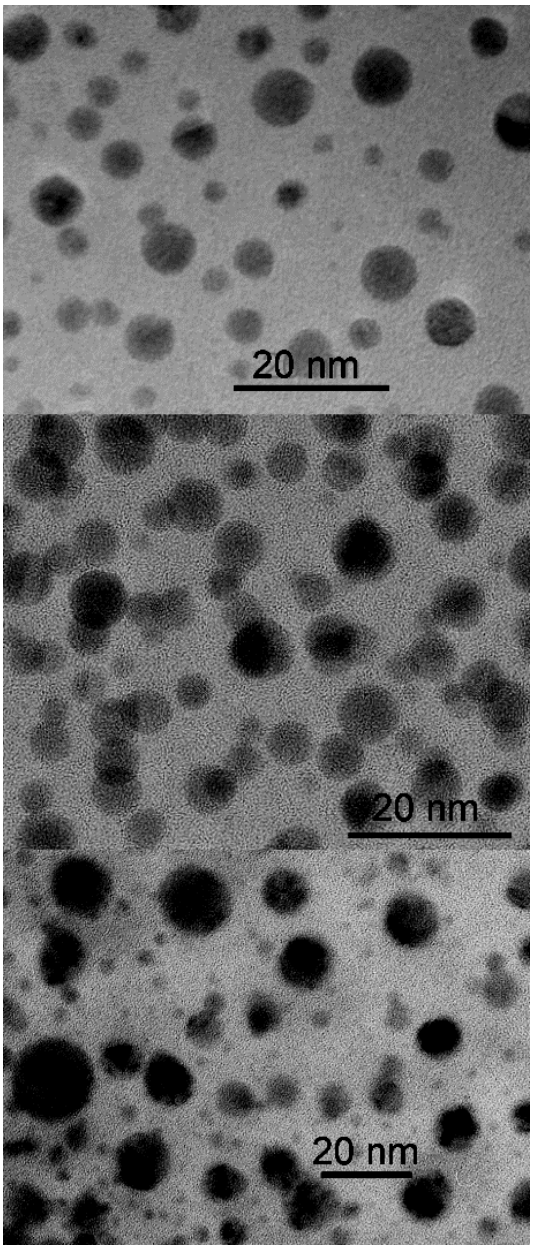

Fig. 2. Example TEM images of Au particles in Sample 2 for (from top to bottom) before laser treatment; after laser treatment with 532 nm at 110 mJ/cm^2; after laser treatment with 266 nm at 50 mJ/cm^2

Transmission Electron Microscopy (TEM) micrographs using a JEM 1010 of JEOL were taken of the cross-section of the films before and after laser treatment. Using these micrographs the gold nanoparticles were counted and their size measured in order to obtain accurate information about the particle size distribution in the samples. At least 500 nanoparticles were counted in each case. These data were used to obtain histograms of the particle radii.

The extinction spectra in the visible range were measured using an Ocean Optics single-beam fibre-optic spectrophotometer

Grazing-Incidence Small-Angle X-ray Scattering (GISAXS) characterization of some of the samples was performed using a Bruker Diffractometer D8 Discover with General Area Detector Diffraction System (GADDS).

Surface roughness characterization was performed by obtaining topographical images in a noncontact mode of several small areas of each sample by employing an AFM Q-Scope 250 manufactured by Quesant Instrument Corporation. The samples were imaged with a cantilever with a spring constant of 0.3 N/m and a silicon carbide tip of 10 nm radius.

3. Results

Fig. 1 and Fig. 2 show cross-sectional high resolution TEM images of two samples before (top) and after treatment with laser light of 532 nm (centre) and 266 nm (bottom) with the indicated fluences. Sample 1 is 200 nm thick and contains 2 at.% Au and Sample 2 is 400 nm thick and contains 8 at.% Au. These images are just examples. A number of such pictures were processed by counting and measuring the diameter of the gold particles visible in them.

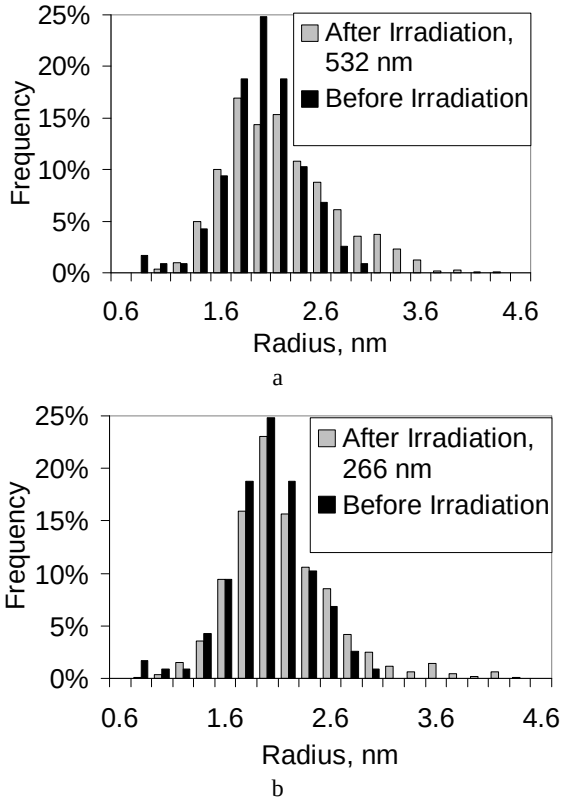

Fig. 3. Size distribution of Au particles in Sample 1: a) comparison of the one before laser treatment with that after laser treatment with 532 nm at 100 mJ/cm^2; b) comparison of the one before laser treatment with that after laser treatment with 266 nm at 50 mJ/cm^2

For each treatment at least 500 particles were counted and measured. This resulted in the histograms shown in Fig. 3 and Fig. 4 where the distribution of particle sizes after each laser treatment is compared to that before the treatment. The results for the mean and volume mean particle sizes derived from the histograms as well as the average size estimated for Sample 2 from the GISAXS experiment are shown in Table 1. It is evident from Fig. 1 and Fig. 2 that on the whole the particles in Sample 2, which contains a higher concentration of Au, are larger. For both samples the visual examination of the TEM images after laser irradiation justifies the conclusion that the size of the particles does not change significantly as a result of the laser treatment. After laser treatment of both samples, the particles keep their spherical shape and exhibit no elongation. Comparison of the histograms of particle sizes before and after the laser treatment with 532 nm and 266 nm for the two samples shows that there is a slight tendency for an increase of the number of larger particles and decrease of the number of smaller particles after laser treatment.

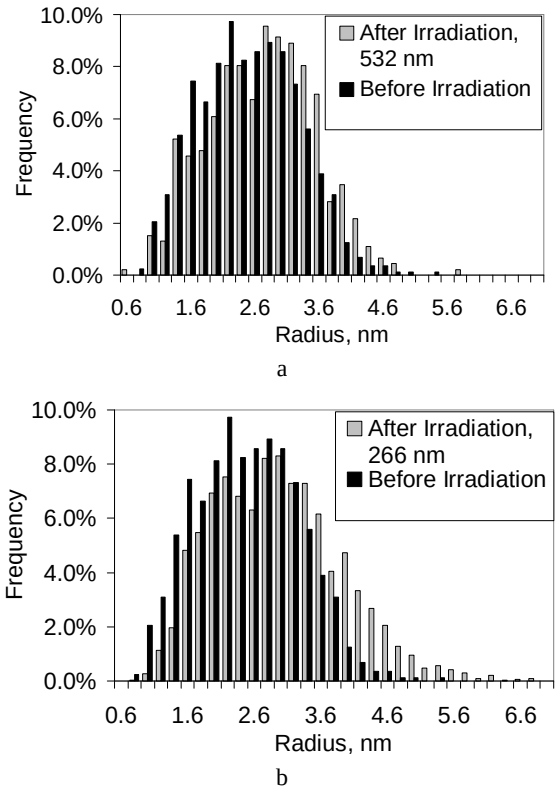

Fig. 4. Size distribution of Au particles in Sample 2: a) comparison of the one before laser treatment with that after laser treatment with 532 nm at 110 mJ/cm^2; b) comparison of the one before laser treatment with that after laser treatment with 266 nm at 50 mJ/cm^2.

This is evident from the mean and volume mean radii calculated from the histograms summarized in Table 1. For Sample 1, which has a smaller metal content, there seems to be no significant difference in the result of the treatment with the two laser lines. For Sample 2 the irradiation with the 266 nm line has a stronger effect on the size of the particles. The same tendency is observed in the GISAXS data.

Fig. 5 exhibits the surface plasmon resonance (SPR) extinction spectra of the studied samples before laser irradiation and after each of the laser treatments. The SPR extinction band for Sample 1 changes in intensity but does not change significantly in width after each laser treatment (Fig. 5a). In the case of the sample with higher concentration of Au, Sample 2 (Fig. 5b), there is a significant drop in the intensity of the spectrum after each laser treatment as well as a broadening of the lower energy wing.

Table 1. Results for the average particle sizes determined in different ways. S1 and S2 are Sample 1 and Sample 2, respectively. R_M is the mean particle radius and R_V is the volume average radius, both calculated from the respective histogram with an error less than 0.05 nm. R_{GISAXS} is the mean radius determined by the GISAXS experiment with an error of 0.1 nm.

Sample and treatment	Thickness [nm]	Au content [at. %]	R_M [nm]	R_V [nm]	R_{GISAXS} [nm]
S1 Before treatment	200	2	1.9	2.0	-
S1 After laser 532 nm	-	-	2.1	2.2	-
S1 After laser 266 nm	-	-	2.0	2.2	-
S2 Before treatment	400	8	2.4	2.6	2.9
S2 After laser 532 nm	-	-	2.6	2.9	3.2
S2 After laser 266 nm			2.9	3.2	3.4

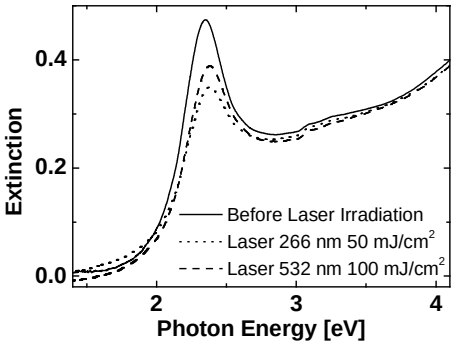

a

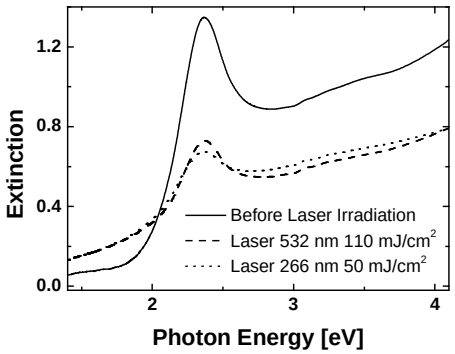

b

Fig. 5. Experimental extinction spectra as indicated in the figure for a) Sample 1; b) Sample 2

This can be attributed to absorption and scattering by defects connected with the considerable damage to the layer observed by optical microscopy reaching the point of opening holes in it. However, in both cases no considerable change in the mean size of the nanoparticles responsible for the resonance can be inferred from the optical extinction spectra, which is in accord with the TEM data.

Atomic force microscopy images of Sample 2 surface topography after laser irradiation with two different fluences (60 mJ/cm^2 and 130 mJ/cm^2) of the 532 nm laser light are shown in Fig. 6. At the lower fluence the surface roughness has an rms of 80 nm and 600 nm periodic structures are observed. The height difference of the ripples is between 60 nm and 90 nm. At the higher laser fluence, Fig. 6b, the surface roughness is increased and there is no periodic structure formation.

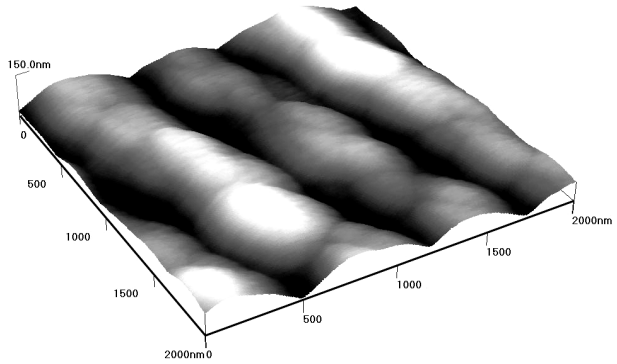

a

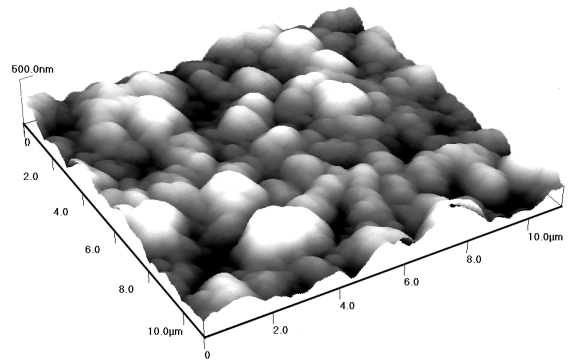

b

Fig. 6. Atomic force microscopy images of Sample 2 surface topography after laser irradiation with two different fluences of the 532 nm laser line a) 60 mJ/cm^2 and b) 130 mJ/cm^2

4. Discussion

The study of the effect of the laser irradiation on the surface morphology of the thin silica films containing gold nanoparticles (Fig. 6) indicates that above a certain threshold fluence the laser irradiation unavoidably alters the surface topography. Although the incident laser irradiation is not absorbed by the silica matrix, but only by the embedded metal nanoparticles, there is enough energy transformed into heat to increase the surface roughness by up to a factor of 20, from rms of 4 nm to rms of 80 nm. The self-organized, laser induced 600 nm periodic structures are a result of melting and re-solidifying of the surface layer due to a periodic temperature pattern. The periodic temperature gradient is a result of interference between the incident and the scattered irradiation along the surface of the film. Since the incident beam is linearly polarized, the interference is maximized for scattered beams with polarizations parallel to the incident beam. Gratings, like this ripple structure, support the propagation of waves with electric field vectors along the ripples. The latter are formed parallel to the polarization of the incident radiation. The process is self-organized since it starts from isotropic surface scattering, in the presence of a selective positive feedback, leading to the formation of a well defined periodic structure. The plane polarization of the incident radiation is the selection factor controlling the positive feedback. Such periodic pattern with a single beam exposure is not observed with nonpolarized irradiation. In earlier studies we have reported similar structures on polymer surfaces [8] created by the fourth harmonic of Nd:YAG irradiation and on $Ag:SiO_2$ by the second harmonic of Nd:YAG irradiation [6]. The threshold fluence for inducing ripples was estimated to be around 40 mJ/cm^2, and it depends on the absorption coefficient of the sample under irradiation. The periodicity of the structure is directly related to the wavelength of the incident radiation and the direction of the ripples is parallel to the plane of polarization of the laser irradiation. At higher laser fluences, Fig. 6b, the surface roughness increases and there is no periodic structure formation. We have not observed ripples when the films were exposed to irradiation with a wavelength of 266 nm. The only effect when the films were irradiated with 266 nm light is the increase of the surface roughness without the formation of any type of periodic pattern. As discussed in our previous study [8] the surface tension of the softened or molten surface plays a critical role for the formation of the periodic pattern. The surface tension of the material in molten state resists ripple formation with a spatial period below a certain threshold. This can explain the fact that no ripple formation was observed when the silica film surface was irradiated with 266 nm light.

The photons absorbed by the gold nanoparticles can induce several processes: 1) Heating the nanoparticles; 2) A metal nanoparticle can eject monomers or dimers due to excitation of its vibrational modes after absorption of laser light – a process called dissociation, which has been observed for free particles or nanoparticles on a surface [9,10]; 3) Another possible mechanism of fragmentation is through ionization of a nanoparticle, leading to surface charging which in turn causes it to disintegrate into smaller particles as a result of electrostatic repulsion forces [11]. Dissociation energies of metal nanoparticles are smaller than their ionization energies [12], and are reported to converge to the cohesive energy of the corresponding bulk metal [10], which is 3.79 eV for gold [13]. One 266 nm (4.66 eV) photon would be enough to supply that energy. However, at least two 532 nm photons would be needed for the dissociation process. Ionization of a gold nanoparticle would require at least two 266 nm photons and more than two 532 nm (2.33 eV) photons if we use the work function of bulk gold - 5.1 eV as an estimate of the ionization energy [13]. As processes requiring fewer photons are more probable than higher order ones, the 266 nm line would be naturally more effective in gold particle dissociation and ionization. For the same reason dissociation would be the more probable process as it requires fewer photons. The excess energy of the excited electrons after photon absorption is dissipated by equilibration with the lattice of the metal particles and later through energy transfer from the hot electron/phonon system to the surrounding matrix [14], which is heated as a result.

In summary, the photon absorbtion by gold nanoparticles in the film can be divided into three possible channels - 1) after absorption by the electrons most of the energy is passed to the vibrational modes through equilibration, thus heating the particles and the surrounding matrix; 2) a smaller portion of the energy goes for dissociation of the particles; and 3) an even smaller part goes for ionization of some of the particles and the following fragmentation. The probability of ionization is low since at least two 266 nm or three 532 nm photons are needed for it to take place.

As the absorbed energy is proportional to the volume of the particle and the energy dissipated to the matrix proportional to the particle surface, larger particles, having larger volume to surface ratio, are heated to a higher temperature than smaller ones. Besides, when the concentration of the metal is higher the distances between the particles are smaller, the heat fluxes from them combine to heat the matrix to a higher temperature. Such collective heating phenomena are reported by other groups [5,15]. The appearance of the ripples on the surface of the films is only possible if there is a melting of the matrix during and shortly after the laser pulse. Therefore, the lack of change in the mean size of the nanoparticles is not a consequence of insufficient heating. In fact, the film as a whole is heated so much through heat diffusion from the particles and from absorption by defects created in the matrix that we can expect that the observed effects are predominantly of thermal nature - similar to those taking place during thermal annealing. As a consequence, the small, but detectable increase of the number of larger particles at the expense of the smaller ones can be attributed to Ostwald ripening. In our particular case we can call this process photo-stimulated Ostwald ripening to distinguish it from the purely thermal process occurring during annealing of the films in a furnace at high

temperature. It is well known that atoms on the surface are energetically less stable than those already well ordered and packed in the interior. Overall, smaller nanoparticles (radii less than 1.6 nm), for which the ratio of surface to inner volume atoms is between 1 and 0.5 tend to be energetically more unstable in comparison to larger particles. Therefore, ions and atoms from the smaller particles have the tendency to dissolve and precipitate on the larger particles in order to minimize the total cohesive energy of the system [16]. When the 266 nm line is used, in addition to the heat generated by optical absorption, the process of dissociation becomes very probable as only one photon is needed and it should contribute to the growth of larger particles at the expense of smaller ones. The combined effects of the photon energy sufficient to trigger the dissociation process, the availability of larger gold particles, and the higher gold concentration lead to a detectable increase of the mean size of the particles in Sample 2 (Fig. 4b).

5. Conclusions

Laser treatment with the second and fourth harmonic of a Nd:YAG laser with 5 ns pulses with a frequency of 10 Hz and fluences between 50 and 130 mJ/cm^2 leads to a very small change in the mean size of the gold nanoparticles of radius between 2 and 3 nm embedded in silica matrix. The increase of surface roughness and the appearance of ripples on the sample surface after laser treatment prove that surface melting of the films occurs during the laser pulse. Cracks are observed after laser treatment especially in the film with higher Au concentration. Although, the size distribution of gold nanoparticles of small sizes (less than 5 nm) is relatively stable under laser irradiation, at higher gold concentration, the film as whole is damaged by the treatment. A small but observable increase of the mean radius is registered and it is attributed to Ostwald ripening of the bigger particles at the expense of the smaller ones - a process facilitated by the heating of the film and photostimulated dissociation of nanoparticles.

Acknowledgements

This work was supported by NSF-INT collaborative research grant OISE 0354463. The authors are grateful to Dr. Orlin Angelov for depositing the films used in this study and to Dr. Kurt Erlacher for the GISAXS measurements. M.S. thanks Rose Ruther, Thomas Hartsfield, Robin Jacobs-Gedrim, and Vesta Zhelyaskova for their help with some of the particle statistics.

References

[1] O. Dammer, B. Vlckova, M. Slouf, J. Pfleger, Mater. Sci. Eng. B **140**, 138 (2007)
[2] N. Satoh, H. Hasegawa, K. Tsujii, K. Kimura, J. Phys. Chem. **98**, 2143 (1994)
[3] F. Bonneau, P. Combis, J.L. Rullier, J. Vierne, M. Pellin, M. Savina, M. Broyer, E. Cottancin, J. Tuaillon, M. Pellarin, L. Gallais, J.Y. Natoli, M. Perra, H. Bercegol, L. Lamaignère, M. Loiseau, J.T. Donohue, Appl. Phys. B **75**, 803 (2002)
[4] S.I. Kudryashov, S.D. Allen, S. Papernov, A.W. Schmid, Appl. Phys. B **82**, 523 (2006)
[5] H. H. Richardson, Z. N. Hickman, A. O. Govorov, A. C. Thomas, W. Zhang, M. A. Kordesch, Nano Lett. **6**, 783 (2006)
[6] M. Sendova, M. Sendova-Vassileva, J.C. Pivin, H. Hofmeister, K. Coffey, A. Warren, J. Nonosci. Nanotechnol. **6**, 748 (2006)
[7] M. Sendova-Vassileva, M. Sendova, A. Troutt, Appl. Phys. A **81**, 871 (2005)
[8] H. Hiraoka, M. Sendova, Appl. Phys. Lett. **64**, 563 (1994).
[9] T. Götz, M. Bergt, W. Hoheisel, F. Träger, M. Stuke, Appl. Surf . Sci. **96-98**, 280 (1996)
[10] U. Hild, G. Dietrich, S. Krückeberg, M. Lindinger, K. Lützenkirchrn, L. Schweikhard, C. Walther, J. Ziegler, Phys. Rev. A 57, 2786 (1998).
[11] P.V. Kamat, M. Flumiani, G.V. Hartland, J. Phys. Chem. B **102**, 3123 (1998).
[12] U. Kreibig, M. Vollmer, Optical Properties of Metal Clusters, Springer Ser. Mater. Sci. 25, Springer, Berlin, Heidelberg (1996).
[13] D.R. Lide, Handbook of Chemistry and Physics, 77th ed., CRC Press, Boca Raton, Florida (1996)
[14] M. Hu, G. V. Hartland, J. Phys. Chem. **106**, 7029 (2002).
[15] A. O. Govorov, W. Zhang, T. Skeini, H. Richardson, J. Lee, N.A. Kotov, Nanoscale Res. Lett. **1**, 84 (2006).
[16] L. Ratke, P.W. Voorhees, Growth and Coarsening: Ostwald Ripening in Material Processing, Springer, Heidelberg (2002).

*Corresponding author: marushka@phys.bas.bg